Porphyrin–Lipid Stabilized Gold Nanoparticles for Surface Enhanced Raman Scattering Based Imaging

ARTICLE *in* BIOCONJUGATE CHEMISTRY · AUGUST 2012

Impact Factor: 4.51 · DOI: 10.1021/bc300214z · Source: PubMed

6 AUTHORS, INCLUDING:

Natalie Tam
University of Toronto
6 PUBLICATIONS **74** CITATIONS
SEE PROFILE

Arash Farhadi
California Institute of Technology
4 PUBLICATIONS **83** CITATIONS
SEE PROFILE

Brian C Wilson
University of Toronto
341 PUBLICATIONS **8,131** CITATIONS
SEE PROFILE

Gang Zheng
Zhejiang University
171 PUBLICATIONS **3,234** CITATIONS
SEE PROFILE

Bioconjugate Chemistry

Communication

pubs.acs.org/bc

Porphyrin–Lipid Stabilized Gold Nanoparticles for Surface Enhanced Raman Scattering Based Imaging

Natalie C. M. Tam,[†,‡] Patrick Z. McVeigh,[†,§] Thomas D. MacDonald,[†,∥] Arash Farhadi,[†,§] Brian C. Wilson,[†,§] and Gang Zheng*[,†,‡,§,∥]

[†]Ontario Cancer Institute, Campbell Family Cancer Research Institute, and Techna Institute [‡]Institute of Biomaterials and Biomedical Engineering, [§]Department of Medical Biophysics, and [∥]Department of Pharmaceutical Sciences, University of Toronto, Toronto, Ontario, Canada

Supporting Information

ABSTRACT: A porphyrin–phospholipid conjugate with quenched fluorescence was utilized to serve as both the Raman dye and a stabilizing, biocompatible surface coating agent on gold nanoparticles. Through simple synthesis and validation with spectroscopy and confocal microscopy, we show that this porphyrin–lipid stabilized AuNP is a novel SERS probe capable of cellular imaging. To date, this is the first use of porphyrin as a Raman reporter molecule for SERS based imaging.

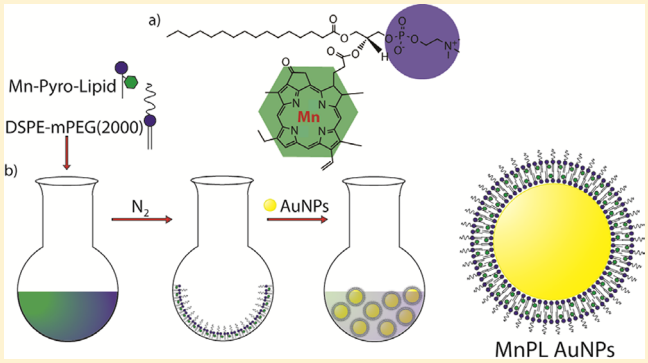

INTRODUCTION

Raman spectroscopy has translated from molecular analysis of chemicals to molecular imaging due to its capacity for molecular identification, photostability, and multiplexing capability.[1,2] In particular, surface enhanced Raman scattering (SERS) techniques based on metallic nanoparticles such as gold (AuNPs) have further advanced its utility for molecular diagnostic imaging by augmenting, by orders of magnitude, the intensity of the inelastically scattered photons, allowing ultrasensitive levels of detection.[1,3] With AuNPs, the SERS probes are inert, show low toxicity,[4] and can be functionalized with targeting moieties and tuned for near-infrared (NIR) wavelengths to facilitate in vivo imaging.[3,5]

Currently, gold nanostructures for SERS imaging and sensing have been based on chromophores adsorbed onto the metallic surface and subsequently encapsulated by various surface coatings to improve biocompatibility and stability. Such Raman dyes commonly contain symmetrical moieties, such as pyrrole or benzene rings, that have strong Raman-active modes due to the double bonds being highly polarizable.[6] Dyes are either selected for or modified to contain functional groups (e.g., thiol –SH) that allow for chemi- or physi-adsorption to metallic surfaces; however, they may have altered affinities in the presence of differing surrounding biological matrix,[7] likely from competing thiols or oxidation.[8] To date, several different classes of surface coating, namely, poly(ethylene glycol) (PEG) and silica, have produced stable SERS probes for in vitro and in vivo imaging.[3,5,9] Recently, our group designed Raman active phospholipid gold nanoparticles (RAP AuNPs), a biocompatible and versatile alternative that shows both structural and Raman signal stability, using phospholipid as a surface coating.[10] Although robust, RAP AuNPs follow a similar synthetic strategy as previous SERS probes, where the initial step of loading dye molecules onto the AuNPs gives rise to concentration- and dye-dependent inconsistencies[11] in the Raman signals that may lead to uncontrolled aggregation and ultimately result in low reproducibility.[12,13]

In the present study, we combined a phospholipid with a chromophore to coat AuNPs, thereby both providing SERS detection capabilities and conferring structural stability and biocompatibility. We have previously reported synthesis of a porphyrin–lipid conjugate using a near-infrared (NIR) photosensitizer, pyropheophorbide-a,[14,15] linked to a single acyl chain phospholipid, 16:0 lysophosphatidylcholine, at the glycerol backbone. We have demonstrated that these conjugates (pyro-lipid or PL) can self-assemble into bilayer nanoparticles, yielding phototherapeutic and imaging functions.[16,17] Porphyrins have strong Raman scattering due to their heterocyclic pyrrole structure and can be enhanced by both electromagnetic and charge transfer to exhibit SERS spectra.[18] However, the Raman signal is usually overwhelmed by the endogenous fluorescence. Although metal-free or closed-shell metal-inserted porphyrins are fluorescent, chelation of open-shell metal ions (e.g., Cu^{2+} or Mn^{3+}) within the planar structure quenches the fluorescence. This ability to chelate divalent metallic ions on pyro-lipid was also previously demonstrated with Cu^{2+} loaded

Received: April 16, 2012
Revised: August 3, 2012
Published: August 9, 2012

   dx.doi.org/10.1021/bc300214z | *Bioconjugate Chem.* 2012, 23, 1726–1730

pyro-lipid, which maintained bilayer stacking assembly and could serve as positron emission tomography (PET) imaging contrast agents.[19] It is also known that chelation of Mn^{3+} can convert a porphyrin from a fluorescent sensor to an MRI contrast agent.[20] Hence, inserting suitable metal ions into porphyrins could eliminate fluorescent interference with the Raman signals, as well as introducing multimodal imaging functionality.

RESULTS AND DISCUSSION

Here, we report successful development of a porphyrin−lipid conjugate with quenched fluorescence by Mn^{3+} that confers biocompatibility to the AuNP surface and stabilizes the nanoparticles in various aqueous buffers, as well as acting as a Raman reporter. Unlike conventional methods where surface agents are used to encapsulate the pre-Raman dye adsorbed gold nanoparticle, we have simplified the synthesis of these SERS probes by using a phospholipid−chromophore conjugate acting both as the Raman reporter and protective surface coating. At the same time, we eliminate the necessity of selecting specific dyes only suitable for adsorption to AuNPs and provide a more reproducible strategy to obtain consistent Raman intensities for making SERS probes.

Scheme 1. Structure of Manganese Pyro-Lipid (MnPL) (a) and Three-Step Procedure for Creating SERS AuNPs with MnPL (b)

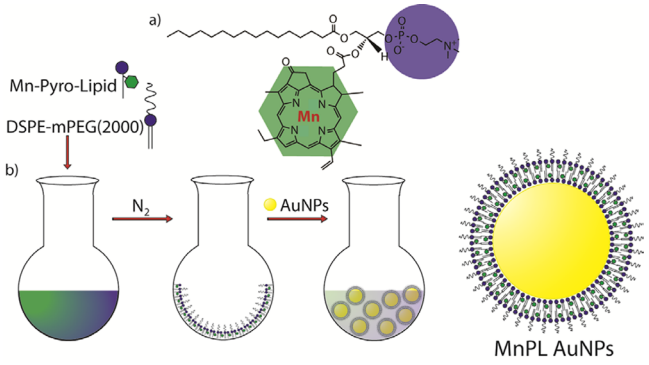

The conjugation of pyropheophorbide-a to 1-palmitoyl-2-hydroxy-*sn*-glycero-3-phosphocholine and the method of subsequent manganese chelation onto the pyro-lipid (MnPL) are described in detail elsewhere.[16] The resulting MnPL has quenched fluorescence, as expected (Supporting Information Figure 1). As shown in Scheme 1, MnPL is mixed with PEGylated phospholipids (1,2-distearoyl-*sn*-glycero-3-phosphoethanolamine-*N*-[methoxy(polyethylene glycol)-2000]) in a 1:1 ratio in chloroform and dried as a lipid film under N_2 gas in a round-bottom flask. The lipid film is directly hydrated with 60 nm AuNPs suspended in distilled H_2O. As for any energetically favorable conformation with phospholipids, direct hydration often creates multilamellar vesicles; thus, the MnPL-AuNP composites are further modified by vortexing, sonication, and subsequent rounds of centrifugation to ensure uniform phospholipid coating and that any free vesicles without any entrapped gold nanoparticles are removed. The resulting structure can be seen in Figure 1a, where the transmission electron microscopy (TEM) image shows a clear phospholipid coating of 4−7 nm.

To assess whether the MnPL coating also acts as a Raman reporter, we characterized the purified solution using a Raman spectrometer operating at 785 nm excitation (Figure 1b). Comparing this spectrum with Raman spectra from resonance Raman scattering of similar metallo-porphyrins,[21] each of the prominent peaks at 751 cm^{-1}, 986 cm^{-1}, 1138 cm^{-1}, 1228 cm^{-1}, 1327 cm^{-1}, and 1531 cm^{-1} were closely matched, confirming that the observed spectrum displayed the pyropheophorbide-a within the nanoparticle assembly. This clearly demonstrates that Mn^{3+} loaded pyropheophorbide-a situated within the lipid coating is detectable by Raman

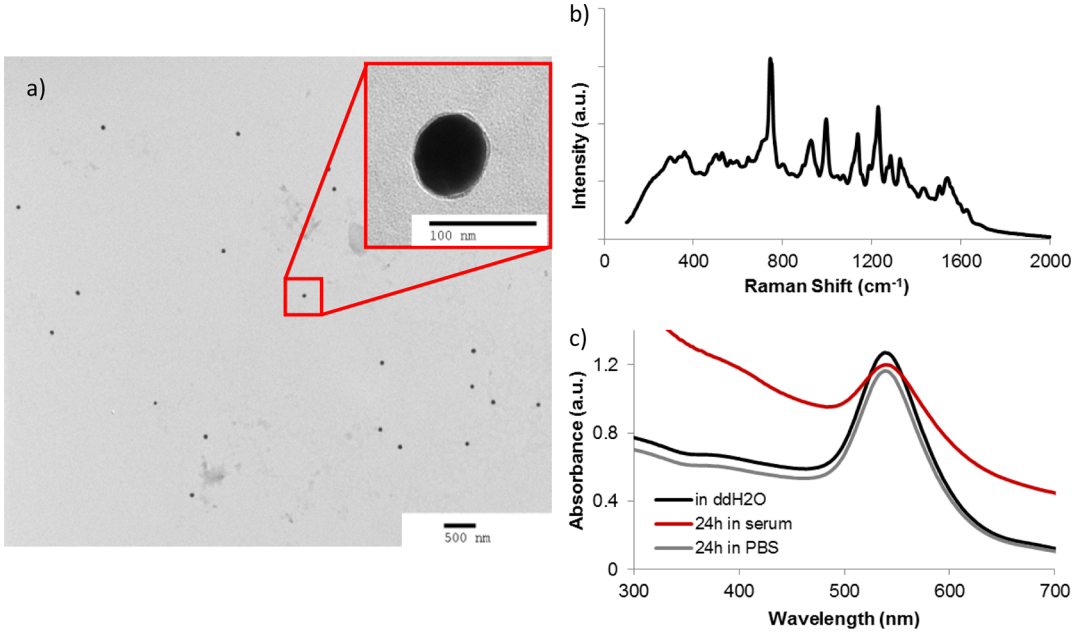

Figure 1. TEM image (a) of MnPL AuNP showing full coverage of pyro-lipid surrounding the AuNP surface with thickness of 4−7 nm. Surface enhanced Raman spectrum (b) of MnPL AuNPs with 785 nm laser (75 mW, 1 s). (c) UV−vis spectra of MnPL AuNPs after 24 h in differing buffers (distilled water (ddH_2O), serum, and phosphate buffered saline (PBS)) a 37 °C.

dx.doi.org/10.1021/bc300214z | *Bioconjugate Chem.* 2012, 23, 1726−1730

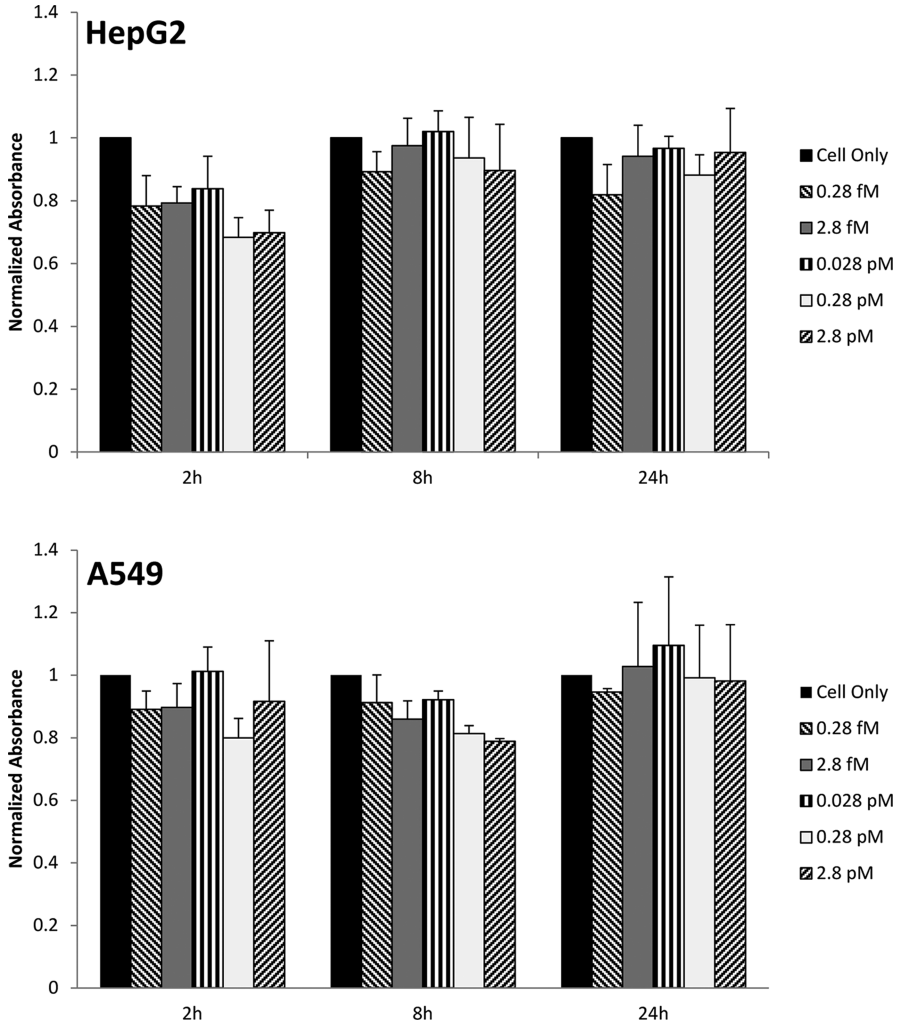

Figure 2. Cytotoxicty of MnPL AuNPs on HepG2 and A549 human cell lines determined by MTT assay. The relative cell viability was normalized to untreated cells for varying NP concentrations and incubation times. Error bars represent mean value ± standard deviation of three independent experiments, each performed in triplicate.

spectroscopy and that it does not require the Raman dye be adsorbed onto the AuNP surface. Moreover, we specifically identified this as a surface-enhancement effect from its interaction with the AuNP surface and not due any excessive free porphyrins or pyro-lipid in solution, since no Raman signal could be detected from MnPL in solution at over 1000× concentration in the absence of AuNPs (Supporting Information Figure 2).

As expected, the use of MnPL as surface coating conferred outstanding biocompatible stability, similar to that from phospholipid coating alone.[10] As seen in Figure 1c, there was no shift in the absorption maximum (λ_{max} = 542 nm) of MnPL AuNPs after 24 h in either phosphate buffered saline (PBS) or 50% fetal bovine serum (FBS) solution. The lack of any red shift of the absorption peak demonstrates that the MnPL is sufficient to prevent AuNP aggregation from serum proteins and at physiological ion concentrations. There is a broadening of the absorption peak for nanoparticles in serum, which is likely due to the protein corona expected to adhere on their surface.[22,23]

We investigate the effect of MnPL AuNPs on the viability of different human cell lines at doses that are believed to be in the range likely encountered in vivo, namely 1−100 gold nanoparticles per cell.[24] The cytotoxicity of MnPLAuNPs to different cell lines was assessed by using MTT assay. Human liver hepatocellular carcinoma HepG2 cell line was chosen to test the MnPL toxicity to liver cells since gold nanoparticles have high accumulation in the liver,[24] while the human non-small cell lung cancer A549 cell line was selected as the target cell line for SERS molecular imaging. As shown in Figure 2, no significant toxicity was observed in either HepG2 or A549 cells incubated with MnPL AuNPs at concentrations of 0.28 fM, 2.8 fM, 28 fM, 0.28 nM, 2.8 nM (1, 10, 100, 1000, 10000 NP/cell, respectively) for 2, 8, and 24 h. The low cytotoxicity of MnPL AuNP was also confirmed on two other cell lines (Supporting Information Figure 3).

We further analyzed the MnPL AuNPs as a SERS imaging probe by incubating MnPL AuNPs with A549 cells for 1 h at 37 °C and subsequently imaging by confocal Raman microscope. The AuNPs were removed and cells were washed repeatedly with PBS and fixed with 4% paraformaldehyde. Confocal Raman microscopy maps was taken with 785 nm excitation with an integration time of 250 ms at each 5 μm step. The pseudocolored image shows the signal intensity corresponding to the peak at 1239 cm^{-1} (Figure 3b). The differential interference contrast (DIC) image (Figure 3a) shows intracellular and extracellular clusters of AuNPs that coincide with regions of peak SERS intensity in the corresponding Raman

dx.doi.org/10.1021/bc300214z | *Bioconjugate Chem.* 2012, 23, 1726−1730

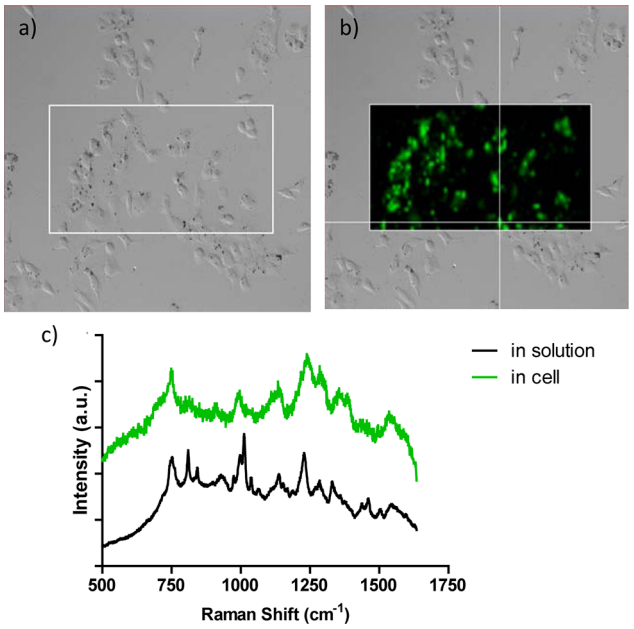

Figure 3. DIC (a) and Raman (b) microscopy images of A549 lung cancer cells showing MnPL AuNP used for cellular imaging. Images were captured using 785 nm laser illumination and displaying the intensity at 1239 cm^{-1}. Point spectrum measurements (c) of MnPL AuNPs in cells (green) at the crosshairs shown in (b) compared with MnPL AuNPs in solution (black) with 785 nm laser at 3 mW integrated for 250 ms.

map (Figure 3b). Although the MnPL AuNPs were incubated for a relatively short time, it is not surprising that they are detected both on the periphery and inside the cells, since A549 cells display active nonspecific endocytosis.[25] Comparing the spectrum between MnPL AuNPs in solution with that spectrum within the cells, there is both an increase in background intensity and a broadening of specific peaks (Figure 3c). The former is likely due to the fixation and mounting reagents used to preserve cell structure for microscopy, which have a weak fluorescence at 785 nm excitation. These additional molecules may also be within the SERS enhancement field, leading to smaller additional peaks and broadening of the existing peaks of the MnPL AuNPs. It cannot be ruled out that the broadening of the Raman peaks may be in part from molecular changes due to aggregation of pH-induced effects from endosomal uptake. Nevertheless, it is clear that, through the combination of porphyrin−lipid on AuNPs to create MnPL AuNPs, porphyrins do function as an effective Raman reporter for SERS imaging.

In summary, we have demonstrated a novel strategy to create SERS probes by combining a phospholipid surface coating with a chromophore. This will expand the selection of dyes that can be used for Raman multiplex detection, since they no longer require specific thiol groups for adsorption to the AuNP surface. In addition, this approach streamlines the synthesis, provides stability, and reduces the variability due to the uncontrollable amount of Raman dye needed to first adsorb to gold nanostructures prior to surface functionalization. To our knowledge, this is the first use of porphyrin as a Raman reporter molecule for SERS based molecular imaging. The use of Mn-based porphyrins not only eliminates the fluorescence background, but also creates unique intrinsic multimodal imaging (optical plus magnetic resonance) and therapeutic capabilities.

In the past decade, there has been increased interest in the clinical use of label-free Raman spectroscopy to delineate cancerous specimens in situ with remarkable specificity and sensitivity,[26,27] while an alternative strategy has been to introduce SERS nanoprobes that target cancer biomarkers as molecular imaging agents to confer diagnostic sensitivity and specificity in vivo. The unique spectral fingerprint of SERS nanoprobes allows for easy differentiation of SERS signal from background noise from the biological sample, as well as multiplexed imaging of multiple SERS contrast agents in vivo. Work done by Nie et al. has shown sensitivity of SERS contrast agents for detecting target cancer cells in mouse whole blood cells (WBC) at levels greater than 10^4:1 WBC to cancer cell.[28] This investigation prompted an institutionally approved clinical trial detecting circulating tumor cells in SCCHN patients. Furthermore, studies conducted by Gambhir et al. have shown the utility of SERS contrast agents to delineate tumor margins from healthy tissue in brain cancer bearing animal models.[29] This has shown the potential of SERS optical contrast agents to aid surgical resection and help reduce the recurrence of cancer resulting from remaining cancer cells. With improvements to the signal strength, biocompatibility, and development of new instrumentation, optical imaging using SERS contrast agents is showing promising and exciting utility for in vivo molecular imaging in the clinical setting.

■ ASSOCIATED CONTENT

Supporting Information

Detailed experimental methods, fluorescence quench of pyro-lipid by Mn chelation, demonstration of the lack of Raman signal from free MnPL at over 1000× concentration of that used in MnPL AuNP, and additional MTT assay results. This material is available free of charge via the Internet at http://pubs.acs.org

■ AUTHOR INFORMATION

Corresponding Author

*Correspondence to Dr. Gang Zheng, 101 College Street, TMDT 5-363, Toronto, Ontario M5G 1L7, Canada. Tel: 416-581-7666; Fax: 416-581-7667; E-mail:gang.zheng@uhnres.utoronto.ca.

Notes

The authors declare no competing financial interest.

■ ACKNOWLEDGMENTS

This work was supported by Natural Science and Engineering Research Council of Canada, Canadian Institute of Cancer Research, Canadian Foundation for Innovation, Princess Margaret Hospital Foundation and the Joey and Toby Tanenbaum/Brazilian Ball Chair in Prostate Cancer Research.

■ REFERENCES

(1) Kneipp, J., Kneipp, H., and Kneipp, K. (2008) SERS - a single-molecule and nanoscale tool for bioanalytics. *Chem. Soc. Rev. 37*, 1052−1060.

(2) Zavaleta, C. L., Smith, B. R., Walton, I., Doering, W., Davis, G., Shojaei, B., Natan, M. J., and Gambhir, S. S. (2009) Multiplexed imaging of surface enhanced Raman scattering nanotags in living mice using noninvasive Raman spectroscopy. *Proc. Natl. Acad. Sci. U. S. A. 106*, 13511−6.

(3) Qian, X., Peng, X. H., Ansari, D. O., Yin-Goen, Q., Chen, G. Z., Shin, D. M., Yang, L., Young, A. N., Wang, M. D., and Nie, S. (2008)

In vivo tumor targeting and spectroscopic detection with surface-enhanced Raman nanoparticle tags. *Nat. Biotechnol. 26*, 83−90.
(4) Thakor, A. S., Luong, R., Paulmurugan, R., Lin, F. I., Kempen, P., Zavaleta, C., Chu, P., Massoud, T. F., Sinclair, R., and Gambhir, S. S. (2011) The fate and toxicity of Raman-active silica-gold nanoparticles in mice. *Sci. Transl. Med. 3*, 79ra33.
(5) Jokerst, J. V., Miao, Z., Zavaleta, C., Cheng, Z., and Gambhir, S. S. (2011) Affibody-functionalized gold-silica nanoparticles for Raman molecular imaging of the epidermal growth factor receptor. *Small 7*, 625−33.
(6) Schlucker, S. (2009) SERS Microscopy: nanoparticle probes and biomedical applications. *ChemPhysChem 10*, 1344−1354.
(7) Flynn, N. T., Tran, T. N. T., Cima, M. J., and Langer, R. (2003) Long-term stability of self-assembled monolayers in biological media. *Langmuir 19*, 10909−10915.
(8) Love, J. C., Estroff, L. A., Kriebel, J. K., Nuzzo, R. G., and Whitesides, G. M. (2005) Self-assembled monolayers of thiolates on metals as a form of nanotechnology. *Chem. Rev. 105*, 1103−69.
(9) Zavaleta, C. L., Hartman, K. B., Miao, Z., James, M. L., Kempen, P., Thakor, A. S., Nielsen, C. H., Sinclair, R., Cheng, Z., and Gambhir, S. S. (2011) Preclinical evaluation of Raman nanoparticle biodistribution for their potential use in clinical endoscopy imaging. *Small 7*, 2232−40.
(10) Tam, N. C., Scott, B. M., Voicu, D., Wilson, B. C., and Zheng, G. (2010) Facile synthesis of Raman active phospholipid gold nanoparticles. *Bioconjugate Chem. 21*, 2178−82.
(11) Faulds, K., Littleford, R. E., Graham, D., Dent, G., and Smith, W. E. (2004) Comparison of surface-enhanced resonance Raman scattering from unaggregated and aggregated nanoparticles. *Anal. Chem. 76*, 592−8.
(12) Cialla, D., Marz, A., Bohme, R., Theil, F., Weber, K., Schmitt, M., and Popp, J. (2012) Surface-enhanced Raman spectroscopy (SERS): progress and trends. *Anal. Bioanal. Chem. 403*, 27−54.
(13) McLaughlin, C., Graham, D., and Smith, W. E. (2002) Comparison of resonant and non resonant conditions on the concentration dependence of surface enhanced Raman scattering from a dye adsorbed on silver colloid. *J. Phys. Chem. B 106*, 5408−5412.
(14) Zhang, M., Zhang, Z., Blessington, D., Li, H., Busch, T. M., Madrak, V., Miles, J., Chance, B., Glickson, J. D., and Zheng, G. (2003) Pyropheophorbide 2-deoxyglucosamide: a new photosensitizer targeting glucose transporters. *Bioconjugate Chem. 14*, 709−14.
(15) Lovell, J. F., Liu, T. W., Chen, J., and Zheng, G. (2010) Activatable photosensitizers for imaging and therapy. *Chem. Rev. 110*, 2839−57.
(16) Lovell, J. F., Jin, C. S., Huynh, E., Jin, H., Kim, C., Rubinstein, J. L., Chan, W. C., Cao, W., Wang, L. V., and Zheng, G. (2011) Porphysome nanovesicles generated by porphyrin bilayers for use as multimodal biophotonic contrast agents. *Nat. Mater. 10*, 324−32.
(17) Lovell, J. F., Jin, C. S., Huynh, E., Macdonald, T. D., Cao, W., and Zheng, G. (2012) Enzymatic regioselection for the synthesis and biodegradation of porphysome nanovesicles. *Angew. Chem., Int. Ed. Engl. 51*, 2429−33.
(18) Murphy, S., Huang, L., and Kamat, P. V. (2011) Charge-transfer complexation and excited-state interactions in porphyrin-silver nanoparticle hybrid structures. *J. Phys. Chem. C 115*, 22761−22769.
(19) Shi, J., Liu, T. W., Chen, J., Green, D., Jaffray, D., Wilson, B. C., Wang, F., and Zheng, G. (2011) Transforming a targeted porphyrin theranostic agent into a PET imaging probe for cancer. *Theranostics 1*, 363−70.
(20) Zhang, X. A., Lovejoy, K. S., Jasanoff, A., and Lippard, S. J. (2007) Water-soluble porphyrins as a dual-function molecular imaging platform for MRI and fluorescence zinc sensing. *Proc. Natl. Acad. Sci. U. S. A. 104*, 10780−5.
(21) Andersson, L. A., Loehr, T. M., Cotton, T. M., Simpson, D. J., and Smith, K. M. (1989) Spectroscopic analysis of chlorophyll model complexes: methyl ester ClFe(III)pheophorbides. *Biochim. Biophys. Acta 974*, 163−79.
(22) Lundqvist, M., Stigler, J., Elia, G., Lynch, I., Cedervall, T., and Dawson, K. A. (2008) Nanoparticle size and surface properties determine the protein corona with possible implications for biological impacts. *Proc. Natl. Acad. Sci. U. S. A. 105*, 14265−70.
(23) Cedervall, T., Lynch, I., Lindman, S., Berggard, T., Thulin, E., Nilsson, H., Dawson, K. A., and Linse, S. (2007) Understanding the nanoparticle-protein corona using methods to quantify exchange rates and affinities of proteins for nanoparticles. *Proc. Natl. Acad. Sci. U. S. A. 104*, 2050−5.
(24) Boisselier, E., and Astruc, D. (2009) Gold nanoparticles in nanomedicine: preparations, imaging, diagnostics, therapies and toxicity. *Chem. Soc. Rev. 38*, 1759−1782.
(25) Stearns, R. C., Paulauskis, J. D., and Godleski, J. J. (2001) Endocytosis of ultrafine particles by A549 cells. *Am. J. Respir. Cell Mol. Biol. 24*, 108−15.
(26) Molckovsky, A., Song, L.-M. W. K., Shim, M. G., Marcon, N. E., and Wilson, B. C. (2003) Diagnostic potential of near-infrared Raman spectroscopy in the colon: Differentiating adenomatous from hyperplastic polyps. *Gastrointestinal Endoscopy 57*, 396−402.
(27) Zavaleta, C. L., Kircher, M. F., and Gambhir, S. S. (2011) Raman's "effect" on molecular imaging. *J. Nucl. Med. 52*, 1839−1844.
(28) Wang, X., Qian, X., Beitler, J. J., Chen, Z. G., Khuri, F. R., Lewis, M. M., Shin, H. J. C., Nie, S., and Shin, D. M. (2011) Detection of circulating tumor cells in human peripheral blood using surface-enhanced Raman scattering nanoparticles. *Cancer Res. 71*, 1526−1532.
(29) Kircher, M. F., de la Zerda, A., Jokerst, J. V., Zavaleta, C. L., Kempen, P. J., Mittra, E., Pitter, K., Huang, R., Campos, C., Habte, F., Sinclair, R., Brennan, C. W., Mellinghoff, I. K., Holland, E. C., and Gambhir, S. S. (2012) A brain tumor molecular imaging strategy using a new triple-modality MRI-photoacoustic-Raman nanoparticle. *Nat. Med. 18*, 829−834.